This is a repository copy of *Anchored self-similar 3D Gauss-Markov mobility model for ad hoc routing scenarios*.

White Rose Research Online URL for this paper:
https://eprints.whiterose.ac.uk/205730/

Version: Published Version

IET Networks

Special issue
Call for Papers

**Be Seen. Be Cited.
Submit your work to a new
IET special issue**

Connect with researchers and experts in your field and share knowledge.

Be part of the latest research trends, faster.

Read more

IET The Institution of Engineering and Technology

IET Networks

ORIGINAL RESEARCH

Anchored self-similar 3D Gauss-Markov mobility model for ad hoc routing scenarios

George Amponis[1,2] 🟢 📷 | Thomas Lagkas[2] 🟢 📷 | Vasileios Argyriou[3] |

Ioannis Moscholios[4] 🟢 📷 | Maria Zevgara[1] | Savvas Ouzounidis[1] | Panagiotis Sarigiannidis[5]

[1]Department of Research and Development, K3Y Ltd., Sofia, Bulgaria

[2]Department of Computer Science, International Hellenic University, Kavala Campus, Greece

[3]Faculty of Science, Engineering and Computing, Kingston University, London, UK

[4]Department Informatics & Telecommunications, University of Peloponnese, Tripolis, Greece

[5]Department of Electrical and Computer Engineering, University of Western Macedonia, Kozani, Greece

Correspondence

Panagiotis Sarigiannidis, Department of Electrical and Computer Engineering, University of Western Macedonia, Kozani 50100, Greece.
Email: psarigiannidis@uowm.gr

Abstract

Given the observed developments of novel communication modes and the establishment of next-generation cellular networks, mobility modelling and ad hoc routing requirements have emerged. Flying ad hoc networks are key pivots in enabling technological leaps in the domain of on-demand communications, especially in emergency scenarios; as such, resorting to application- and mobility-aware routing is a promising enabler of this emerging set of use cases. This article investigates swarm mobility modelling, and applicable routing protocols, conducting comparative analysis that leads to the introduction of the new Anchored Self-Similar 3D Gauss-Markov Mobility Model (ASSGM-3D), which incorporates a novel set of spatio-temporal statistical metrics.

KEYWORDS

ad hoc networks, mobile ad hoc networks, wireless mesh networks

1 | INTRODUCTION

Building upon the outputs of our work entitled 'Swarm Mobility Models and Impact of Link State Awareness in Ad Hoc Routing,' presented in the 13th International Symposium on Communication Systems, Networks and Digital Signal Processing [1], we investigate the potential of Flying ad hoc networks (FANETs) in enabling a new spectrum of next-generation Internet of things applications and introduce a new mobility modelling technique for ad hoc routing applications. Both 5G and 6G cellular networks promise higher density networks, effectively unifying cellular and non-cellular technologies under one uniform architecture [2, 3]. To sustain modern applications sufficiently, 6G will use three-dimensional networks, which can be facilitated in an on-demand manner by means of FANETs. One can subsequently deduce that ad hoc, and especially aerial communications are an integral part of next-generation novel communication applications [4]. Moreover, satellite communications and UAVs can work cooperatively with terrestrial IoT to support high-throughput and low-latency services in heterogeneous and distributed networks. Additionally, with the advent of novel high-density industrial applications and smart, interconnected vehicles, aerial networks can support the extension of terrestrial network coverage and capacity, as well as the assistance of mobile and vehicular ad hoc networks (MANETs/VANETS).

Furthermore, network advancements have a lot of potential for forming dependable communication links in rural and/or isolated locations with little to no existing infrastructure; this is envisaged to help rural revitalisation, smart farming, and can help reduce the digital divide. Aerial base station deployment is

a viable solution to a variety of issues that plague terrestrial IoT networks, such as wireless sensor networks (e.g. ad hoc WSNs). As aerial nodes can be effectively deployed in such a manner that reduces shadowing and blockage effects, they can contribute to the mitigation of signal attenuation and losses in wireless links. Aerial base stations can be deployed to provide reliable and efficient uplink and downlink for device-to-device and IoT-specific communications. Without properly planned location of all communicating nodes in the 3D space, connectivity enhancements and terrestrial network capacity increases will be impossible. Therefore, awareness of node location and accurate mobility modelling is critical. This is need is highlighted true in the case of power-constrained devices, as they require their respective gateways to be placed to that they can use the minimum possible required transmission power [5].

Eliciting optimal routing algorithms and methods is important to optimise connectivity provision and obtain the most efficient end-to-end routes. Ad hoc routing protocols typically are not aware of all nodes' link states (existence or lack thereof), and only rely on awareness of nodes' immediate neighbours' link-states to choose or disregard a potential packet route. However, there exist other types of protocols which involve the periodical broadcasting of link states to all participating nodes. This supports a more intelligent and table-driven approach to routing, at the cost however of some additional overhead and bandwidth utilisation. Figure 1 showcases a relaying use case, where mobility and path selection effectiveness are of utmost importance.

In view of these challenges, this paper aims to contribute towards the establishment of a holistic view in regards to the interconnection of mobility models, link state-awareness in the context of routing protocols, and the overall communication quality and efficiency. An experiment was conducted in the context of this research, and the results are envisaged to constitute stepping stones for future research in environment-, channel-, and mobility-aware routing.

This work is relevant to 5G/B5G and 6G networks, as it considers and employs an algorithm to model the mobility of aerial nodes participating in a next-generation cellular network in the scope of extending connectivity through relaying. B5G and 6G cellular communications are expected to be significantly enabled by communication relaying via drones. In areas where conventional cel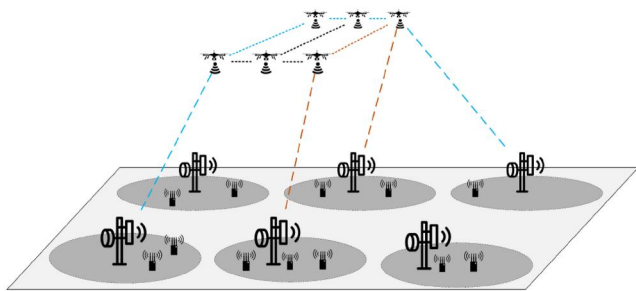lular towers cannot reach, drones can serve as aerial base stations and provide coverage. Drones can be used to fill coverage gaps and offer a solution for areas with weak signal strength or sparse network infrastructure, due to the increasing demand for high-speed Internet and reliable connectivity. Drones can also be deployed to quickly establish a communication network and assist first responders in emergency situations. By operating as a relay, drones can increase the cellular network's capacity and range, facilitating the deployment of B5G and 6G technologies. As a result, it is anticipated that using drones for communication relaying will revolutionise the way we communicate and make advanced cellular technology more widely available in the years to come. Considering those remarks, this work builds on existing research in ad hoc communications and relevant applicable mobility models to offer a new, more optimised solution for modelling such scenarios where drones are employed.

Drawing inspiration from the recurrent self-similar Gauss-Markov mobility model [6], we evaluate the behaviour of two routing protocols of interest in different mobility scenarios and eventually introduce a new anchored self-similar 3D Gauss-Markov-based mobility model. By doing so, we target the research gap present in the domain of accurately modelling and representing application-specific mobility vectors of aerial nodes. More specifically, we aim to accommodate communications relaying scenarios for emergencies. The proposed self-similar anchored mobility model accurately describes the behaviour of drone swarm, considering metrics and variables associated with a given node's spatio-temporal parameters. Effectively, the proposed methodology renders nodes reluctant to shift their momentum and angular velocity in respect to their previous states and when acceleration is increased, something which accurately describes the behaviour of a swarm during a such targeted scenario. Similarly, authors in [7] propose the random destination with pheromone zone mobility model for reconnaissance applications. Their model works by dividing the area of interest into zones in order to reduce the issue to an imbalance problem.

It is important to note that the existing state-of-the-art mobility models for ad hoc networks, including FANETs, have several limitations that restrict their effectiveness in accurately representing the mobility patterns of aerial nodes participating in communication relaying and cellular connectivity 'daisy-chaining'. These limitations arise from the complex dynamics of aerial vehicles engaging in this complex process, such as the effects of wind, turbulence, and changes in altitude, which have a significant impact on the performance of communication relaying. Traditional models, such as the aforementioned Random Walk and Gauss-Markov models, are unable to account for these complex dynamics, resulting in suboptimal performance in terms of packet delivery ratio and end-to-end delay. The limitations of these models have created a need for new mobility models that can accurately capture the complex dynamics of aerial nodes and facilitate efficient communication relaying.

In this paper, we build upon the work presented in our previous publication [1] by introducing a new and improved mobility model that better represents the movement of aerial

FIGURE 1 Mobility and route-sensitive flying ad hoc network relaying scenario.

nodes in ad hoc networks. Our previous work focused on evaluating the performance of networked nodes using traditional mobility models, while the main contribution of this paper is the introduction of the anchored self-similar 3D Gauss-Markov mobility model, which incorporates a novel set of spatio-temporal statistical metrics. The ASSGM-3D model is designed to accurately model the complex behaviour of drone swarms. Overall, our work provides a novel and effective approach to modelling the movement of aerial nodes in ad hoc networks.

2 | METHODS—MOBILITY MODELS FOR DRONE SWARMS

Mobility models are of utmost importance for the analysis and effective simulation and modelling of drone swarms, and mobile ad hoc networks in general. There exist several mobility models to approximate the movement of nodes in a swarm network. This section analyses a number of such mobility models, with the ultimate purpose of eliciting a set of realistic and not overly computationally-demanding models for simulating and benchmarking multi-hop communications in FANETs.

Firstly, there exists the Gauss-Markov mobility model, which attempts to accommodate various mobility randomness levels. This model assumes that velocity vectors of various swarm nodes are completely independent. Swarm nodes are initially assigned a defined direction and velocity. At constant intervals, both velocity and direction are updated using a randomiser, also considering previous velocity and direction. Consideration of previous node velocity and direction is typically successful in mitigating possible abrupt path alterations [8]. This model is mature and well-researched in the context of drone swarms; there also exists a variant of this model called 3D Gauss-Markov, specifically developed for multi-altitude FANETs, as it considers and randomises mobility in all three dimensions [9]. Considering the fundamental functionality of this model, authors in [10] proposed an Enhanced Gauss-Markov mobility model, to facilitate realistic modelling for FANETs. This model incorporates mechanisms to eliminate/limit abrupt stops and sharp turns within the simulation region.

Secondly, there exists the Semi Random Circular mobility model, which attempts to accommodates curved and circular trajectories. This makes the model applicable in the context of patrolling and inspection applications, and military/repetitive surveillance operations in general security. The semi-random circular mobility model has proven to be more efficient than existing models for the simulation of curved manoeuvring, since it is the first one specifically designed for curved scenarios [11].

Thirdly, there exists the Random Waypoint mobility model [12]. This model is capable of simulating node motion based on linear motion and its derivatives (turns, stops). It considers and models the location, velocity and acceleration change of a swarm node. In this model, each node defines a random destination, within a predefined grid, and then engages it at a random velocity. This method does not incorporate any predefined paths for the movement of individual nodes. Should the node achieve this defined goal, it pauses for a random amount of time (within predefined constrains), and then defines a new destination. The process then repeats itself. Thanks to its low computational complexity and overall algorithmic simplicity, it is one of the most popular mobility models for mobile ad hoc networks.

Fourthly, there exist the Particle Swarm mobility model. This model tries to maintain a collision-free swarm node distribution at all times by considering the spatial relationship amongst networked nodes. The first step implemented by this algorithm is the logging of the node velocities and waypoints. Then, for each node, the model generates new velocity vectors and waypoints. Lastly, the particle swarm mobility model performs various adjustments in the velocity vector of swarms nodes, to avoid collisions, and the process is repeated for every waypoint. This model succeeds in keeping all UAV nodes in safe distances, while achieving high temporal and spatial correlation and guaranteeing path availability [13]. This makes the model suitable for the modelling of intelligent swarms, composed of predicatively manoeuvring nodes.

Fifthly, there exists the Paparazzi mobility model which incorporates a total of five possible node manoeuvres, namely 'stay-at', 'waypoint', 'eight'', 'scan' and 'oval' [14]. Combinations of those five aforementioned basic manoeuvres are capable of covering virtually all realistic node movements in the three-dimensional space. This model is ideal for simulating manoeuvring of multi-node swarms. It provides an accurate description of a swarm's mobility in a real-life environment thanks to the combination of a realistic number of commonly-used manoeuvres.

The aforementioned mobility models are all of high value for the analysis and simulation of UAV swarms' behaviour and even link quality estimation, as each one describes the behaviour of a network engaging in different tasks. Table 1 summarises the main advantages and possible application scenarios

TABLE 1 Mobility models.

Mobility model	Advantages	Use case
Gauss-Markov	No sudden path alterations, prediction of node positions.	Search-and-rescue
Semi random circular	Realistic aerial	Patrolling
Random waypoint	Computationally simple, long-lived links	Relaying
Particle swarm	Realistic collision avoidance, realistic path planning	Patrolling
Paparazzi	Simple manoeuvre modelling	Search-and-rescue

for which each mobility model would provide sufficient simulation realism and accuracy. The two highlighted mobility models chosen for the evaluation we implemented are the Gauss-Markov and the random waypoint models, due to heir heterogeneity and diverse application scenarios. In the chosen simulator (NS3), using a mobility model involves several steps:

1) Selecting a mobility model: NS3 provides several built-in mobility models, including Random Walk, Random Direction, Gauss-Markov, and Constant Position models. Alternatively, one can use a custom mobility model that has been developed independently.

2) Configuring the mobility model: Once a mobility model has been selected, one will need to configure its parameters, such as the initial position, velocity, and acceleration. Depending on the specific model, one may also need to configure additional parameters, such as the turning radius or maximum speed.

3) Assigning the mobility model to nodes: After configuring the mobility model, one will need to assign it to the nodes in the network. In NS3, this is typically done using the `Set Position Allocator` and Instal methods.

4) Running the simulation: Once the mobility model has been assigned to the nodes, the simulation can be run in order to observe how the nodes move over time. One can also collect data on various metrics, such as the distance between nodes or the number of packet transmissions.

In order to use a mobility model in NS3, one must first choose and set up the model, then assign it to nodes and run the simulation to watch how the network behaves. A realistic mobility model must be included in order to effectively describe the behaviour of mobile nodes in NS3, which offers a versatile and potent framework for simulating the behaviour of wireless networks.

3 | ROUTING PROTOCOLS FOR DRONE SWARMS

In the survey presented in ref. [15], we discuss matters of routing for FANETs in high detail. In the context of the work at hand, we will place focus on a small slice of the routing protocols analysed and compared in the aforementioned work. This section is dedicated to the analysis of routing protocols' attributes, and their impact on the overall throughput of FANETs. This section also analyses the potential impact of link state awareness in the packet delivery rate (PDR) in a FANET. In the context of this paper, we will consider state-awareness as table-based link state-awareness.

3.1 | Stateful routing

Stateful routing in mobile ad hoc networks involve each node periodically broadcasting routing table updates to update the corresponding cache containing routes to and from each networked node. Stateful routing protocols are pro-active and the corresponding protocols have pre-determined paths stored in the form of a cached routing table.

A perfect example of stateful table-driven ad hoc routing protocol is Optimised Link State Routing (OLSR). Optimised link state routing is a proactive (table-driven), and topology-based, link-state aware routing protocol. It utilises a hop-by-hop approach to facilitate packet routing. Its predominant advantage over other routing protocols is decreased message overhead. Optimised link state routing achieves a substantial overhead decrease by resorting to contained flooding using multi-point relays (MPRs), reducing unnecessary transmissions occurring in an already covered range of the network. Multi-point relays are used to forward packets and flood broadcasted control messages, effectively reducing re-transmissions. An MPR node must be a direct neighbour to the node whose packets it forwards and its range shall cover other two hop nodes (with respect to the source-node). The default implementation of OLSR three main message types, namely HELLO messages (associated with link sensing, neighbouring node detection and MPR signalling), Topology control messages (associated with topology declaration and control thereof), and MID messages (associated with the declaration of the existence of multiple interfaces).

It is important to note however, that link state awareness in the context of the default implementation of OLSR can only sense the presence and not the quality of an existing link. Many promising attempts have been made towards enabling link quality awareness. A great such example is the work of R. Jain and I. Kashyap [16], who attempted to evaluate link quality by using incoming TCP acknowledgements (ACKs) and comparing them to the expected ones while considering the expected transmission count (ETX) metric which regards packet forwarding probability and probability of ACK reception. In theory, this link state-aware routing protocol should be capable of outperforming non-link state-aware protocols in non-violently shifting topologies, in terms of consistency. This is to be expected, as link states are broadcasted throughout the network, and as such inactive routes can be proactively excluded from the cached forwarding table of individual nodes.

3.2 | Stateless routing

Stateless routing in mobile ad hoc networks involve the on-demand (reactive) routing computation and generation of packet routes. Nodes participating in stateless routing only carry and are concerned with local information about their immediate neighbours. Stateless routing protocols typically rely on the information received from one-hop neighbours for void detection and bypassing during routing.

A great such example is the Ad-hoc On-demand Distance Vector Routing (AODV) protocol. AODV computes all routes on-demand, with no route optimisation being implemented by default (since link states are not available to all networked nodes). Lack of link state awareness implies that packets are routed through the same path until it can no longer be used.

Nevertheless, route optimisation can be implemented through the usage of link-layer feedback or by proactively enabling HELLO-message based re-routing, suggested by B. Deokate, Ch. Lal, D. Trček, and M. Conti [17]. The stateless AODV protocol uses the four main message types, namely HELLO messages (used to maintain links amongst neighbours), Route Request (RREQ) (broadcasted right before transmission), Route Reply (RREP) (informing the node about to transmit of the route to the packet's destination), and Route Error (REER) (used to inform the transmitting node of a failed link).

Considering that AODV lacks the capability to inform its nodes of the state of all participants' links through periodical broadcasts (as is the case with stateful protocols) it benefits from reduced route setup delay. However, lack of global link state awareness introduces potential congestion and removes the possibility for the implementation of route optimisations.

4 | RESULTS—ROUTING PROTOCOLS AND MOBILITY MODELS COMPARATIVE ANALYSIS

This section compares and analyses the simulation conducted in the context of the research and hand. To compare the impact of node mobility and global link state awareness, we devised an NS3-based simulation framework, involving the measurement of the two candidate protocols' (OLSR and AODV) performance under two highly diverse mobility models. For this comparative analysis, we chose the Gauss-Markov mobility model and the Random Waypoint mobility model. This mobility model choice is deliberate, as they are perfect examples for the analysis of swarm behaviour in two distinct scenarios. This approach is complementary to the hardware testbed-based methodology we suggested in [18]. Additional analysis on physical deployments will benefit the scope of this research, as it would enable the elicitation of conclusions based on even more representative mobility- and channel-related metrics.

The simulation parameters are described in Table 2. The total number of nodes has been set to 20, and the number of sinks to 10. As a propagation loss model, we considered the Friis free space propagation model. In this manner, we effectively model the path losses introduced along the line-of-sight (LOS) of the assumed free space environment (no absorption/diffraction/reflections-inducing objects between nodes). The MAC standard we considered is 802.11b which operates on a 2.4 GHz band. Channel throughput is assumed to be equal to 2 kb/s, which is assumed to be realistic for the considered scenario. To introduce some challenge in the establishment and maintenance of inter-swarm links, node velocity is assumed to be equal to 20 m/s (72 km/h). This high velocity will allow us to benchmark the capability of each routing protocol to maintain viable communication links in high-speed environments. Similarly, the unique characteristics of the Random Waypoint and the Gauss-Markov mobility models will be significantly highlighted, and more valuable results will be obtainable under high, yet realistic, speeds. Figure 2 showcases

TABLE 2 Simulation parameters.

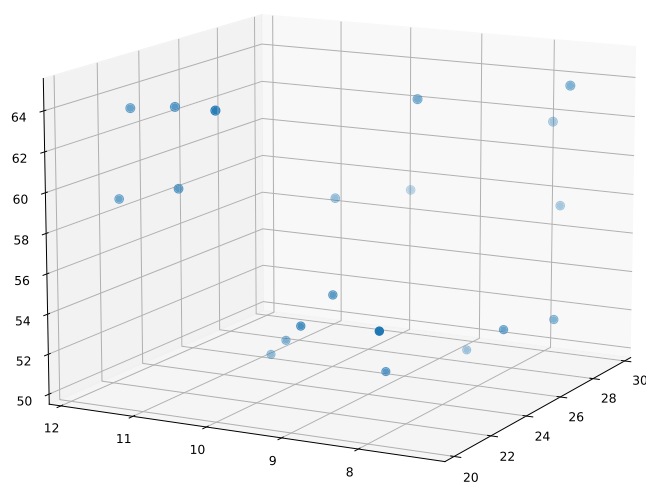| Attribute	Value
Number of nodes	20
Number of sinks	10
Propagation loss model	Friis
Position allocator	Random rectangular position
MAC standard	802.11b
Throughput	2 kb/s
Simulation time	120 s
Node velocity	20 m/s
Node pause time	0.25 s
Network address	10.1.1.0/24
Mobility models	Gauss-Markov, random waypoint
Routing protocols	OLSR, AODV

FIGURE 2 Initial positions of 20 aerial nodes in the 3D space.

the approximate starting positions of the 20 nodes participating in the routing experiment.

In the first scenario, we tested both OLSR and AODV under the Gauss-Markov mobility model, in terms of the achieved PDR. Figure 3 compares the aforementioned metric graphically, using the parsed outputs of NS3, concerning successful packet reception.

A quick observation is that PDR under this mobility model is initially dropped to approximately 1% and then rises almost linearly. This can be attributed to the Gauss-Markov model's idiosyncrasy, and inherent consideration of previous locations to derive future ones. It can be deduced that as time passes, more stable PDR will be achievable by both protocols. Moreover, it can be observed that both protocols performed relatively poorly, with peak PDR reaching 14% in the case of AODV, and 10% in the case of OLSR. This relatively low PDR can be attributed to the high node mobility we introduced in the context of this comparative analysis. Nevertheless, once swarm links have been established, OLSR performed more

consistently, and with fewer sudden peaks and drops, which characterise AODV.

By analysing the captured pcap files and creating flow figures, we drew more conclusions. Figure 4 showcases the performance of OLSR under the currently analysed mobility model. The figure shows the packet rate in intervals of 10 s. On average, OLSR under Gauss-Markov managed to achieve on average, roughly 5 packets per 10 s, translating to 0.5 packet per second. Figure 5 similarly showcases the performance of AODV under Gauss-Markov. Contrary to OLSR, AODV appeared to perform measurably better and more consistently, achieving on average, roughly 10 packets per 10 s, correspondingly translating to 1 packet per second.

In the second scenario, we tested both OLSR and AODV under the random waypoint mobility model, in terms of the

achieved PDR. Figure 6 graphically compares the PDR metric graphically.

It can be observed that AODV's zero-overhead route setup shows a measurable benefit in the start of the routing process. Furthermore, In that case, OLSR appears to offer a less consistent PDR. Contrary to the first scenario, passage of time did not improve the performance of the routing protocols. This is because the random waypoint mobility model does not consider previous node positions to compute the new ones. Subsequently, peak PDR of both protocols was less than that in the previous scenario. AODV achieved a peak of 12%, while OLSR achieved a peak PDR of 8.5%.

As is the case with the first scenario, we captured and analysed the traffic exchanged between the nodes through flow plots. Figure 7 showcases the performance of OLSR under the random waypoint mobility model. In this case packet rate drops almost immediately after the alteration of the initial node positions. On average, OLSR achieved 6 packets per 10 s, equal to 0.6 packets per second under this model. Figure 8 showcases the performance of AODV, which follows roughly the same pattern, only with a somewhat increased packet rate: 13 packets per 10 s, equal to 1.3 packets per second on average.

The results presented in this show amongst others, the limitations of the current state-of-the-art mobility models and their impact on the performance of communication relaying in ad hoc networks. Specifically, we observed suboptimal packet delivery ratios for airborne nodes, indicating a need for a new mobility model that can more accurately capture the complex
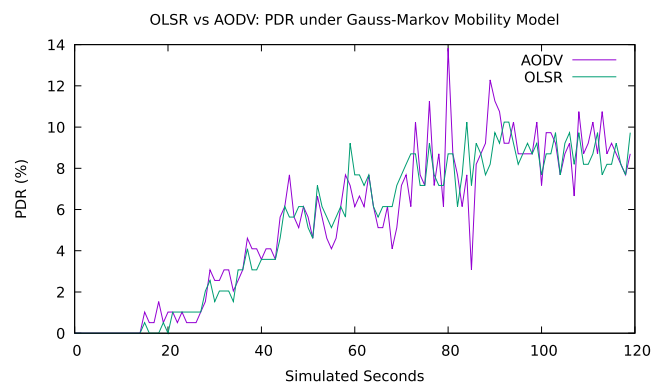

FIGURE 3 Comparison of the packet delivery rate achieved with optimised link state routing and AODV under the Gauss-Markov Mobility Model.
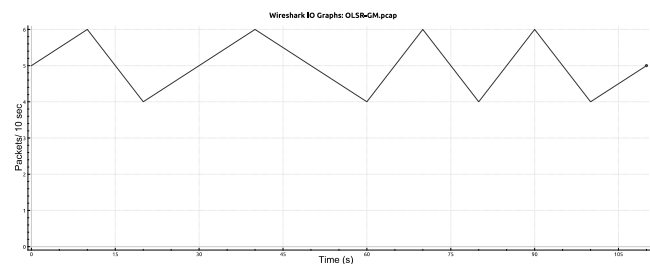

FIGURE 4 Optimised link state routing packet transmission rate under the Gauss-Markov mobility model (10 s interval).
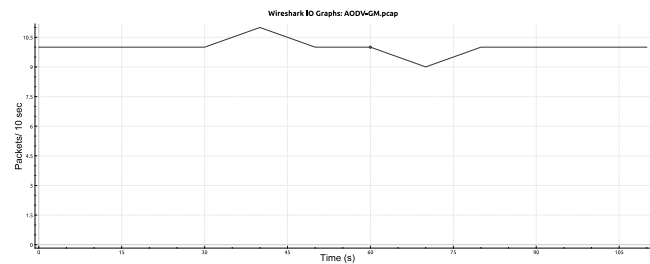

FIGURE 5 AODV packet transmission rate under the Gauss-Markov mobility model (10 s interval).
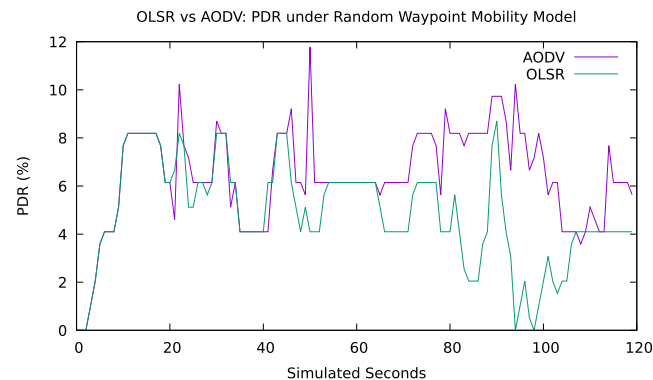

FIGURE 6 Comparison of the packet delivery rate achieved with optimised link state routing and AODV under the random waypoint mobility model.
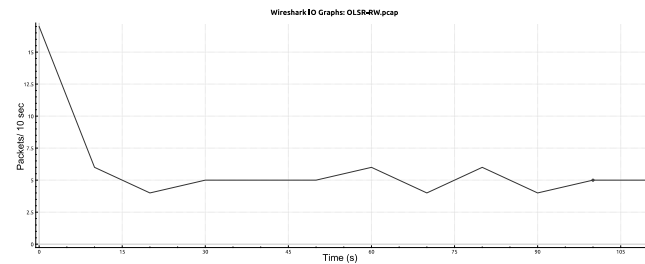

FIGURE 7 Optimised link state routing (OLSR) packet transmission rate under the random waypoint mobility model (10 s interval).
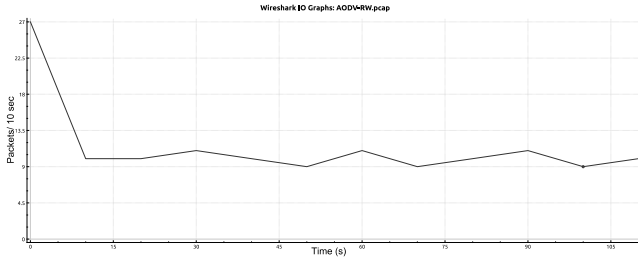
FIGURE 8 AODV packet transmission rate under the random waypoint mobility model (10 s interval).

dynamics of aerial vehicles. In response, we present in the next section a novel anchored self-similar 3D Gauss-Markov mobility model that incorporates a novel set of spatio-temporal statistical metrics, and which can significantly improve the accuracy of mobility modelling for airborne nodes in ad hoc networks. The proposed model is designed to minimise computational load while accurately representing the movement of airborne nodes, thus enhancing the performance of communication relaying in emergency scenarios.

5 | ASSGM-3D: ANCHORED SELF-SIMILAR 3D GAUSS-MARKOV MOBILITY MODEL

In the context of establishing a quantitative means of defining and effectively illustrating various mobility scenarios, we propose a novel application-specific swarm mobility model. Said mobility model is fundamentally based on the basic Gauss-Markov principles and follows a similar deterministic sequential approach. The basic Gauss-Markov mobility model (which is incorporated into NS3), computes three metrics define the new mobility vector of every networked node, for each iteration cycle.

$$s_n = as_{(n-1)} + (1-a)\bar{s} + \sqrt{(1-a^2)}s_{x_{n-1}} \tag{1}$$

Equation (1) [19] shows how the Gauss-Markov mobility model defines the new speed of each node, using a randomness index a, and the previous speed of the node, indicated by $s_{(n-1)}$.

$$d_n = ad_{(n-1)} + (1-a)\bar{d} + \sqrt{(1-a^2)}d_{x_{n-1}} \tag{2}$$

Continuing, 2 [19] outputs the new direction of each node, again introducing a degree of randomness through a, and considering the previous direction $d_{(n-1)}$.

$$p_n = ap_{(n-1)} + (1-a)\bar{p} + \sqrt{(1-a^2)}p_{x_{n-1}} \tag{3}$$

Lastly, Equation (3) [20] gives the new value for the pitch of each affected entity, with some degree of Gaussian randomness through a and considering $p_{(n-1)}$, the previous pitch value.

To achieve effective mobility modelling of drone swarms in a communication relaying scenario, we enhance the above-described model using a set of new metrics. This scenario

finds great applicability in military and emergency-response scenarios. In order to effectively model this randomised and coordinated swarm scenario, we need to examine two cases concerning the a index:

1) Assuming $a = 0$, the model loses all randomness, and the new speed, direction and pitch become direct functions of the previous states. This behaviour is sub-optimal, as a degree of randomness needs to be considered at all times when examining and modelling mobility of nodes in an outdoors scenario, where a spectrum of variables affect nodes' spatio-temporal behaviour.

2) Assuming $a = 1$, is becomes evident from Equations (1)–(3) that the new speed, direction and pitch values will be exactly the same as the previous ones, pivoting the affected nodes in a straight linear path. Again, while this is possible in a controlled and highly deterministic environment, is practically not an observable phenomenon in the targeted application scenarios.

Considering the above remarks, we will redefine the speed, direction and pitch equations accordingly. Continuing, in order to address issues arising in modelling relative speed and position changes, we will introduce a set of new relational metrics.

Regarding the process of computing the new speed of nodes, we consider and introduce the relative velocity between two directly networked nodes as a weighted and exponentially decaying positional index. Equation (4) shows the updated randomness index a_s, which is now multiplied by an exponentially decaying expression. We multiply the randomness index by The expression $e^{-\frac{1}{j}\sum_{n=1}^{n}|s_{n-1}-s_n|/\lambda_1}$, effectively introducing the exponentially decaying variance in relative node velocity. Said expression designates the variance in speed between consecutive velocity values. Replacing a with a_s in Equation (1) will yield Equation (5), which fully describes the relationally self-similar process of setting the new speed for a node using the new enhanced randomness index. The effect observed with this addition is the more fluid and stabilised acceleration of each node when changing velocity states. In practice, this equates to a more position-oriented deployment of the swarm, which is the key enabler of communications relaying.

$$a_s = ae^{-\frac{1}{j}\sum_{n=1}^{n}|s_{n-1}-s_n|/\lambda_1} \tag{4}$$

$$s_n = ae^{-\frac{1}{j}\sum_{n=1}^{n}|s_{n-1}-s_n|/\lambda_1}s_{(n-1)}$$
$$+ \left(1 - ae^{-\frac{1}{j}\sum_{n=1}^{n}|s_{n-1}-s_n|/\lambda_1}\right)\bar{s}$$
$$+ \sqrt{\left(1 - a^2e^{-\frac{2}{j}\sum_{n=1}^{n}|s_{n-1}-s_n|/\lambda_1}\right)s_{x_{n-1}}} \tag{5}$$

Continuing with the calculation of new direction for each node, we have implemented a similar enhancement for the Gaussian randomness index, with the addition of the consideration of node acceleration. Equation (6) shows the updated randomness index a_d, which is (similarly to the first case concerning changes in speed) now multiplied by an exponentially decaying expression $e^{-\frac{1}{j}\sum_{n=1}^{n}|d_{n-1}-d_n|/\lambda_2\frac{\partial s}{\partial t}}$. What this achieves is to minimise sudden direction alterations, as the previously observed variance increases, and further reduce them as acceleration increases. This achieves a form of spatial balancing of individual nodes in relation to their previous directions. Effectively, this smooths the rate at which direction changes whilst also maintaining the Gaussian randomisation attribute of the overarching system. Replacing a with a_d in Equation (2) will yield Equation (7). The later describes the process of setting the new speed for a node using the new enhanced randomness index.

$$a_d = ae^{-\frac{1}{j}\sum_{n=1}^{n}|d_{n-1}-d_n|/\lambda_2\frac{\partial s}{\partial t}} \tag{6}$$

$$
\begin{aligned}
d_n = {} & ae^{-\frac{1}{j}\sum_{n=1}^{n}|d_{n-1}-d_n|/\lambda_2\frac{\partial s}{\partial t}} s_{(n-1)} \\
& + \left(1 - ae^{-\frac{1}{j}\sum_{n=1}^{n}|d_{n-1}-d_n|/\lambda_2\frac{\partial s}{\partial t}}\right)\overline{d} \\
& + \sqrt{\left(1 - a^2 e^{-\frac{2}{j}\sum_{n=1}^{n}|d_{n-1}-d_n|/\lambda_2\frac{\partial s}{\partial t}}\right)}d_{x_{n-1}}
\end{aligned} \tag{7}
$$

Lastly, we re-define and improve the process of computing the new pitch, this time using not only the cumulative average of the previous z axis orientation values, but also considering cumulative average velocity and the rate of change of the node's direction. Equation (8) shows the updated randomness index a_p, now multiplied by the exponentially decaying expression $e^{-\frac{1}{j}\sum_{n=1}^{n}|p_{n-1}-p_n|/\lambda_3\frac{\partial d}{\partial t}}$. Replacing a with a_p in Equation (3) yields Equation (9). The later describes the process of setting the new pitch for a node using the new enhanced randomness index. By resorting to these measures, we have ensured that the pitch's rate of change remains anchored to (i.e. can be expressed as a direct function of) the momentum of the node.

$$a_p = ae^{-\frac{1}{j}\sum_{n=1}^{n}|p_{p-1}-p_n|/\lambda_3\frac{\partial d}{\partial t}} \tag{8}$$

$$
\begin{aligned}
p_n = {} & ae^{-\frac{1}{j}\sum_{n=1}^{n}|p_{n-1}-p_n|/\lambda_3\frac{\partial d}{\partial t}} s_{(n-1)} \\
& + \left(1 - ae^{-\frac{1}{j}\sum_{n=1}^{n}|p_{n-1}-p_n|/\lambda_3\frac{\partial d}{\partial t}}\right)\overline{p} \\
& + \sqrt{\left(1 - a^2 e^{-\frac{2}{j}\sum_{n=1}^{n}|p_{n-1}-p_n|/\lambda_3\frac{\partial d}{\partial t}}\right)}p_{x_{n-1}}
\end{aligned} \tag{9}
$$

The model will repeat the above processes for every mobility axis to eventually output a velocity vector spanning 3 dimensions. Algorithm 1 describes the process of obtaining the velocity vector (and thus the mobility traces), which is repeated for each node. The algorithm receives a set of inputs, namely the mean speed, direction and pitch of the node, the mean and standard deviation of a Gaussian distribution (which are used to compute the randomness index a) and a set of boundaries in the 3D space. The mobility vector of each node in the 3D space is computed by Equations (5), (7) and (9).

Algorithm 1 Compute 3D Mobility Vector

Input:
Mean Speed $\overline{s}$;
Mean Direction $\overline{d}$;
Mean Pitch $\overline{p}$;
Mean of Gaussian distribution `mean`;
Standard Deviation of Gaussian Distribution `std`;
Boundaries $(x_{max}, y_{max}, z_{max})$;
Output: Mobility vector (x, y, z)

```
1:  begin
2:      a ← random.gauss(mean, std)
```
3:      $a_s \leftarrow ae^{-\frac{1}{j}\sum_{n=1}^{n}|s_{n-1}-s_n|/\lambda_1}$
4:      $a_d \leftarrow ae^{-\frac{1}{j}\sum_{n=1}^{n}|d_{n-1}-d_n|/\lambda_2\frac{\partial s}{\partial t}}$
5:      $a_p \leftarrow ae^{-\frac{1}{j}\sum_{n=1}^{n}|p_{p-1}-p_n|/\lambda_3\frac{\partial d}{\partial t}}$
```
6:          Compute s_n(a_s)
7:          Compute d_n(a_d)
8:          Compute p_n(a_p)
```
9:      $\overrightarrow{V}_x \leftarrow (s_n\cos(d_n)\cos(p_n))\widehat{i}$
10:     $\overrightarrow{V}_y \leftarrow (s_n\sin(d_n)\cos(p_n))\widehat{j}$
11:     $\overrightarrow{V}_z \leftarrow (s_n\sin(p_n))\widehat{k}$
12:     $\overrightarrow{V}_{xyz} = \overrightarrow{V}_x + \overrightarrow{V}_y + \overrightarrow{V}_z$
```
13:     mobilityVector.append()
14:     if traces(x, y, z) > boundaries(x_max,
        y_max, z_max)
        then
15:         x ←{center} + (x − x_max)
16:         y ←{center} + (y − y_max)
17:         z ←{center} + (z − z_max)
```

```
18:      V⃗ ← traces(x, y, z).append()
19:  end if
     return V⃗ₓᵧ₂
20:end
```

6 | DISCUSSION

The experiments conducted and documented in our previous work [1] provided valuable insight on how global link state awareness affects communication quality under different types of mobility, corresponding to the behaviour of aerial nodes executing different tasks. In the context of this research, we conducted a series of experiments, effectively benchmarking two ad hoc routing protocols, namely OLSR and AODV, as representatives of protocols featuring global link state awareness, and lack thereof, which is substituted by a zero-overhead path establishment scheme respectively in the case of AODV. The obtained experimental results showed that the impact of global link state awareness is not to be underestimated, especially in the context of deterministic shifting mobility vectors, as demonstrated by the experiment using the Gauss-Markov mobility model.

Link state awareness enabled OLSR to perform much more consistently in almost all test scenarios. Nevertheless, AODV, substituting link state awareness with its zero-overhead route setup process, managed to achieve, on average, higher PDRs, despite being less consistent. The optimal protocol type is highly dependent on the individual use case scenario, and the desired functionality of each relaying network. As a general remark, it can be assumed that real-time and data-sensitive applications would typically benefit from link state awareness. Nevertheless, communications placing focus on real-time services on the other hand, do not measurably benefit from link state awareness, and only suffer from higher route setup delays (and the newly introduced overhead). Future work in this domain can consider the research outputs of this paper to support the optimisation of various protocol attributes, applicable to both analysed routing typologies. Regarding OLSR, after observing the simulation logs, abrupt mobility changes seemed to affect the achieved PDR quite significantly. This can be attributed to the protocols ability to sense link states, but inability to sense link quality. On the other hand, AODV proved to not be affected by topology changes to a such extend. This is due to the fact that AODV nodes only consider the state of the link with their immediate neighbours and do not consider all link states for their route selection process.

Considering the inherent limitations of the previously considered mobility models, and the correspondingly poor demonstrated results in terms of packet delivery ratio in the tested use cases, we have proposed a new anchored Gauss-Markov-based mobility model to better simulate the behaviour of a drone swarm in a communication-relaying scenario.

Lastly, the introduced mobility model successfully represents the ad hoc mobility of aerial nodes, when engaging in communication relaying in a three-dimensional grid, while only minimally increasing computational load. The outputted mobility model has been implemented in NS3 and can be used with other emulation platforms with near-zero overhead.

7 | CONCLUSION

This paper has discussed mobility, link state awareness and route selection implications for aerial networks and consequently introduces a novel three-dimensional, self-similar mobility model leveraging Gaussian randomness to accurately model anchored mobility of swarm nodes. Routing metrics involved in the elicitation of optimal combinations of mobility models and routing algorithms are discussed in detail, in order to provide ground for future cellular connectivity enhancements. This paper has engaged in a thorough comparative analysis of stateful and stateless routing protocols under mobility models for 3D environments. In has been deducted that in high-mobility scenarios, while link state awareness is theoretically an advantage, lack of quality-awareness seemed to trigger a disproportionate amount of packet loss.

Further developments and versions of OLSR would benefit from enabling link quality awareness, and the consideration of such parameters as routing metrics. Consideration of link quality may be an even more important metric compared to link state awareness in highly mobile FANETs. Concluding, this work has provided insight to the internal functionalities and route selection mechanisms observed by two different sets of ad hoc routing protocols, its correlation with mobility, and potential relevant future optimisations.

Concluding, the introduced mobility model facilitates the representation of three-dimensional, anchored and self-similar swarm mobility. It utilises Gaussian randomness to illustrate the behaviour of drones anchored to 3D points while participating in emergency communication relaying. Our model's novelty stems from the usage of intricate statistical metrics to optimise the behaviour of nodes, considering the previous known values of velocity, direction, pitch and the rate of change or cumulative average thereof in the 3D space. The proposed model, has been implemented using NS3 using the mathematical descriptors provided in this paper and is available on GitHub [21].

AUTHOR CONTRIBUTIONS

Georgios Amponis: Conceptualisation; Formal analysis; Investigation; Methodology; Software; Visualisation; Writing – original draft; Writing – review & editing. **Thomas Lagkas**: Conceptualisation; Data curation; Funding acquisition; Methodology; Supervision; Writing – review & editing. **Vasileios Argyriou**: Formal analysis; Resources; Supervision; Validation. **Ioannis Moscholios**: Data curation; Methodology; Supervision. **Maria Zevgara**: Funding acquisition; Project administration; Writing – review & editing. **Savvas Ouzounidis**: Writing – review & editing. **Panagiotis Sarigiannidis**: Conceptualisation; Methodology; Project administration; Supervision.

ACKNOWLEDGEMENTS

CONFLICT OF INTEREST STATEMENT

The authors declare no conflict of interest.

DATA AVAILABILITY STATEMENT

The data that support the findings of this study are available upon request.

NOTES

This publication constitutes an extension of the conference paper entitled 'Swarm Mobility Models and Impact of Link State Awareness in Ad Hoc Routing' [1].

ORCID

George Amponis https://orcid.org/0000-0001-6411-0485
Thomas Lagkas https://orcid.org/0000-0002-0749-9794
Ioannis Moscholios https://orcid.org/0000-0003-3656-277X

REFERENCES

1. Amponis, G., et al.: Swarm mobility models and impact of link state awareness in ad hoc routing. In: 2022 13th International Symposium on Communication Systems, Networks and Digital Signal Processing (CSNDSP), pp. 762–767 (2022)
2. Saad, W., Bennis, M., Chen, M.: A vision of 6g wireless systems: applications, trends, technologies, and open research problems. IEEE Network 34(3), 134–142 (2020). https://doi.org/10.1109/mnet.001.1900287
3. Spyridis, Y., et al.: Towards 6g iot: tracing mobile sensor nodes with deep learning clustering in uav networks. Sensors 21(11), 3936 (2021). [Online]. Available:. https://doi.org/10.3390/s21113936 https://www.mdpi.com/1424-8220/21/11/3936
4. Pliatsios, D., et al.: Drone-base-station for next-generation internet-of-things: a comparison of swarm intelligence approaches. IEEE Trans. Antennas Propag. 3, 32–47 (2022). https://doi.org/10.1109/ojap.2021.3133459
5. Saym, M.M., Mahbub, M., Ahmed, F.: Coverage maximization by optimal positioning and transmission planning for uav-assisted wireless communications. In: 2021 International Conference on Science Contemporary Technologies (ICSCT), pp. 1–4 (2021)
6. Alenazi, M.J.F., et al.: RSSGM: recurrent self-similar Gauss–Markov mobility model. Electronics 9(12), 2089 (2020). [Online]. Available:. https://www.mdpi.com/2079-9292/9/12/2089
7. Jo, Y.-I., Fathoni, M.F., Kim, K.: A new mobility model for multi-UAVs reconnaissance based on partitioned zone. Appl. Sci. 9(18), 3810 (2019). [Online]. Available:. https://www.mdpi.com/2076-3417/9/18/3810
8. Meghanathan, N.: Impact of the Gauss-Markov mobility model on network connectivity, lifetime and hop count of routes for mobile Ad hoc networks. J. Network. 5(5), 509–516 (2010). https://doi.org/10.4304/jnw.5.5.509-516
9. Guillen-Perez, A., Cano, M.D.: Flying ad hoc networks: a new domain for network communications. Sensors 18(10), 3571 (2018). https://doi.org/10.3390/s18103571
10. Biomo, J.-D.M.M., Kunz, T., St-Hilaire, M.: An enhanced Gauss-Markov mobility model for simulations of unmanned aerial ad hoc networks. In: 2014 7th IFIP Wireless and Mobile Networking Conference (WMNC), pp. 1–8 (2014)
11. Wang, W., et al.: A novel mobility model based on semi-random circular movement in mobile ad hoc networks. Inf. Sci. 180(3), 399–413 (2010). [Online]. Available:. https://doi.org/10.1016/j.ins.2009.10.001
12. Kuiper, E., Nadjm-Tehrani, S.: Mobility models for UAV group reconnaissance applications. In: Second International Conference on Wireless and Mobile Communications, ICWMC 2006, vol. 00, pp. 2–8 (2006)
13. Li, X., Zhang, T., Li, J.: A particle swarm mobility model for flying ad hoc networks. In: IEEE Global Communications Conference (GLOBECOM) (2017). [Online]. https://ieeexplore.ieee.org/document/8253966
14. Bouachir, O., et al.: A mobility model for uav ad hoc network. In: 2014 International Conference on Unmanned Aircraft Systems (ICUAS), pp. 383–388 (2014)
15. Amponis, G., et al.: A survey on fanet routing from a cross-layer design perspective. J. Syst. Architect. 120, 102281 (2021). [Online]. Available:. https://www.sciencedirect.com/science/article/pii/S1383762121001934
16. Jain, R., Kashyap, I.: An QoS aware link defined OLSR (LD-OLSR) routing protocol for MANETS. Wireless Pers. Commun. 108(3), 1745–1758 (2019). [Online]. Available:. https://doi.org/10.1007/s11277-019-06494-9
17. Deokate, B., et al.: Mobility-aware cross-layer routing for peer-to-peer networks. Comput. Electr. Eng. 73, 209–226 (2019). https://doi.org/10.1016/j.compeleceng.2018.11.014
18. Amponis, G., et al.: Inter-UAV routing scheme testbeds. Drones 5(1), 2 (2021). [Online]. Available:. https://doi.org/10.3390/drones5010002 https://www.mdpi.com/2504-446X/5/1/2
19. Camp, T., Boleng, J., Davies, V.: A survey of mobility models for ad hoc network research. Wireless Commun. Mobile Comput. 2(5), 483–502 (2002). [Online]. https://onlinelibrary.wiley.com/doi/abs/10.1002/wcm.72
20. NSNAM: Gauss Markov Mobility Model Class Reference (2018). https://www.nsnam.org/docs/release/3.28/doxygen/classns3_1_1_gauss_markov_mobility_model.html
21. Amponis, G.: ASSGM-3D (2022). https://github.com/g-ampo/ASSGM-3D

How to cite this article: Amponis, G., et al.: Anchored self-similar 3D Gauss-Markov mobility model for ad hoc routing scenarios. IET Netw. 12(5), 250–259 (2023). https://doi.org/10.1049/ntw2.12089